

Supported Bilayers

International Edition: DOI: 10.1002/anie.201606603
German Edition: DOI: 10.1002/ange.201606603

Profiling Metal Oxides with Lipids: Magnetic Liposomal Nanoparticles Displaying DNA and Proteins

Feng Wang, Xiaohan Zhang, Yibo Liu, Zhi Yuan (William) Lin, Biwu Liu, and Juwen Liu*

Abstract: Metal oxides include many important materials with various surface properties. For biomedical and analytical applications, it is desirable to engineer their biocompatible interfaces. Herein, a phosphocholine liposome (DOPC) and its headgroup dipole flipped counterpart (DOCP) were mixed with ten common oxides. Using the calcein leakage assay, cryo-TEM, and ζ -potential measurement, these oxides were grouped into three types. The type 1 oxides (Fe_3O_4 , TiO_2 , ZrO_2 , Y_2O_3 , ITO, In_2O_3 , and Mn_2O_3) form supported bilayers only with DOCP. Type 2 (SiO_2) forms supported bilayers only with DOPC; type 3 (ZnO and NiO) are cationic and damage lipid membranes. Magnetic Fe_3O_4 nanoparticles were further studied for conjugation of fluorophores, proteins, and DNA to the supported DOCP bilayers via lipid headgroup labeling, covalent linking, or lipid insertion. Delivery of the conjugates to cells and selective DNA hybridization were demonstrated. This work provides a general solution for coating the type 1 oxides with a simple mixing in water, facilitating applications in biosensing, separation, and nanomedicine.

Enveloping nanomaterials with a lipid bilayer, and thus mimicking cell structure, is a unique way to increase biocompatibility.^[1] The supported lipid bilayer masks the underlying inorganic core, allowing different materials to have a common biointerface. Upon forming this lipid coating, various ligands, such as aptamers, peptides, and antibodies, can be readily conjugated.^[2] Furthermore, lipid bilayers are fluid, allowing dynamic organization of surface ligands for optimal polyvalent binding.^[3] A primary example is coating silica by phosphocholine lipids (PC).^[4] The PC headgroup contains a negatively charged phosphate and a positively charged choline (Figure 1 A), rendering this zwitterionic lipid overall charge-neutral.

Such simple PC lipid wrapping however does not occur on most other oxides, which encompass a diverse range of useful materials. A particularly important example is magnetic iron oxide,^[5–7] which is widely used for drug delivery, imaging, biosensing, and separation.^[8–15] To attach biomolecules to iron oxide, its surface needs to be first coated with hydrophobic

ligands, carbon, or silica.^[10,11,16,17] Efforts have also been made to coat lipid membranes. For example, De Cuyper et al. enveloped a phosphatidylglycerol (PG) bilayer on iron oxide, but the process takes two days of dialysis and ligand exchange.^[18,19] Beyond iron oxide, there are many other important oxides. Thus, a general procedure for their lipid coating and an understanding of their biointerfaces is of highly practical and fundamental importance.



Flipping the PC headgroup dipole produces a choline phosphate (DOCP, Figure 1 B).^[20] This chemistry was recently used as a general adherent for cell membranes.^[21] Herein, we compare ten common oxides by using DOPC and DOCP, and report a simple method for preparing lipid-enveloped oxide nanoparticles (NPs) in aqueous buffers and their bioconjugation.

To have a complete understanding, ten common oxide NPs (SiO_2 , Fe_3O_4 , TiO_2 , ZrO_2 , Y_2O_3 , ZnO , NiO , In_2O_3 , ITO, and Mn_2O_3) were included in this study. These NPs were extensively washed to ensure a clean native oxide surface. Their TEM images are shown in the Supporting Information, Figure S1 and most NPs are below 50 nm (Supporting Information, Figure S2). Our liposomes were prepared by extrusion with an average size of about 100 nm (Supporting Information, Figure S3A). DOPC is nearly charge-neutral, while DOCP is anionic due to an extra charge on the terminal phosphate (Supporting Information, Figure S3B). Using rhodamine (Rh)-labeled liposomes, we confirmed that all these oxide NPs can adsorb these two liposomes (Supporting Information, Figure S4).

After adsorption, the liposomes may further break and wrap the oxides to form supported bilayers, and we are most interested in these cases. To probe liposome breakage, a calcein leakage assay was performed. Inside each liposome, the calcein concentration was about 100 mM, leading to self-quenched fluorescence. Fluorescence enhancement would then indicate calcein leakage and compromised membrane integrity. For each experiment, the background fluorescence was monitored for 5 min before an oxide NP was added. In the end, Triton X-100 was added to fully rupture the liposome to calculate the extent of oxide-induced leakage.

Seven oxides (Fe_3O_4 , TiO_2 , ZrO_2 , Y_2O_3 , ITO, In_2O_3 , and Mn_2O_3) leaked the DOCP liposome but not DOPC (Figure 2 A). SiO_2 is the only one that leaked DOPC but not DOCP (Figure 2 B). Finally, ZnO and NiO leaked both liposomes (Figure 2 C). In most cases, liposomes only leaked partially by the oxides, which may be related to the different surface area and surface properties of the oxides. For this initial study, we are more concerned with whether leakage occurs rather than the extent of leakage.

[*] Prof. Dr. F. Wang

School of Biological and Medical Engineering
Hefei University of Technology, Hefei, Anhui 230009 (China)Prof. Dr. F. Wang, X. Zhang, Y. Liu, Z. Y. Lin, B. Liu, Prof. Dr. J. Liu
Department of Chemistry, Waterloo Institute for Nanotechnology
University of Waterloo, Waterloo, Ontario, N2L 3G1 (Canada)
E-mail: liujw@uwaterloo.ca Supporting information and the ORCID identification number(s) for the author(s) of this article can be found under:
 <http://dx.doi.org/10.1002/anie.201606603>.

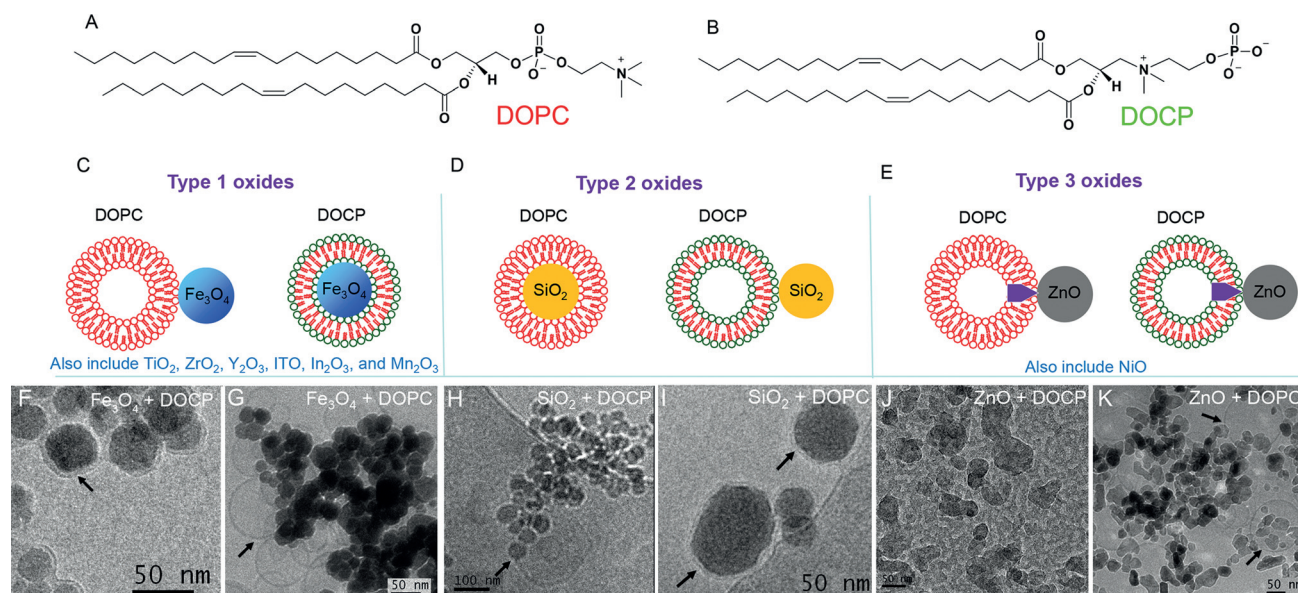


Figure 1. The structures of A) DOPC and B) DOCP lipids. The three types of metal oxides based on their lipid interactions: C) Type 1 includes Fe₃O₄, TiO₂, ZrO₂, Y₂O₃, ITO, In₂O₃, and Mn₂O₃; they are adsorbed by DOPC, but form supported bilayers with DOCP. D) Type 2 includes only SiO₂, forming supported bilayers with DOPC. E) Type 3 includes cationic ZnO and NiO, damaging the membranes (pores indicated by the blue color); full membrane disruption occurs to DOCP when mixed with ZnO. Cryo-TEM images of F), G) Fe₃O₄, H), I) SiO₂, and J), K) ZnO NPs mixed with F), H), J) DOCP or G), I), K) DOCP liposomes. In each sample, the liposomes were added in excess and the free liposomes were removed after centrifugation and washing before cryo-TEM; see the Supporting Information for details. The arrowheads point at the lipid features.

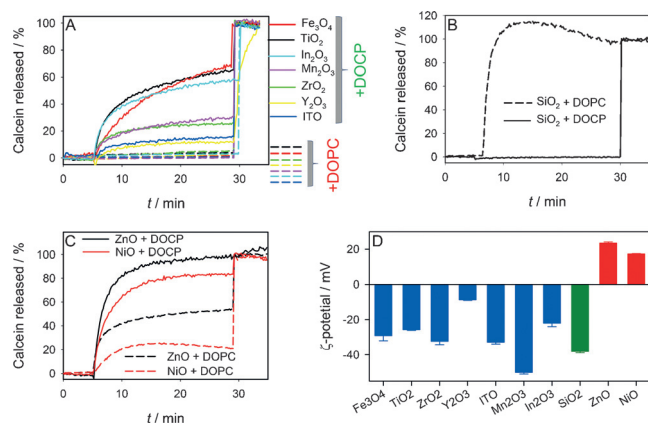


Figure 2. Calcein leakage from the DOPC and DOCP liposomes induced by adding A) Fe₃O₄, TiO₂, ZrO₂, Y₂O₃, ITO, In₂O₃, or Mn₂O₃; B) SiO₂; and C) ZnO and NiO NPs. Solid lines: mixed with DOCP; dashed lines: mixed with DOPC. Oxides were added at 5 min and Triton X-100 at 30 min in buffer (10 mM HEPES, pH 7.4 with 100 mM NaCl), except for In₂O₃, ITO, Mn₂O₃ with 300 mM NaCl. D) ζ -potential of the oxides in 10 mM HEPES, pH 7.4 at 25°C.

To confirm a clean surface, we also freshly prepared Fe₃O₄ NPs in our own lab and they indeed showed a similar leakage profile (Supporting Information, Figure S5). In a separate test, we intentionally capped Fe₃O₄ using citrate to mimic surface contaminated NPs (Supporting Information, Figure S6). In this case, a completely different profile was observed with an induction period that can be attributed to the displacement of the surface citrate by the DOCP liposomes, which in turn confirms that our NPs were not capped by strong ligands.

The leakage experiments suggest that the DOCP liposome might break on many oxides. However, other processes may also cause leakage, such as local pore formation or even full membrane disruption. To further understand this, we carried out cryo-TEM experiment for a few representative oxides.

For the seven oxides in Figure 2A, we chose to study Fe₃O₄, since it is important for many applications and is the focus of this study. We could not find any intact DOCP liposomes (Figure 1F); instead, a circa 5 nm lipid bilayer feature was observed around each Fe₃O₄ NP, confirming supported bilayers and explaining the above calcein leakage data. In sharp contrast, DOPC was adsorbed as intact liposomes (Figure 1G),^[5] which is also consistent with its lack of calcein leakage. Their larger area cryo-TEM images are shown in the Supporting Information, Figures S7, S8. A cartoon describing their interactions is presented in Figure 1C.

SiO₂ leaked DOPC but not DOCP (Figure 2B). It is poorly adsorbed by DOCP liposomes (Figure 1H), while DOPC formed supported bilayers on SiO₂ (Figure 1I).^[5,22] This is exactly opposite to the oxides in Figure 2A (see Figure 1D). This cryo-TEM data can also explain the calcein leakage profile for SiO₂. For the two oxides in Figure 2C, we picked ZnO for its biomedical and optical importance. Interestingly, we observed intact spherical DOPC liposomes (Figure 1K), suggesting the leakage observed in Figure 2C was due to local pore formation at the interface. In contrast to the other tested oxides, which are negatively charged at neutral pH, ZnO and NiO are positively charged (Figure 2D). Many cationic materials induce defects in PC lipid bilayers,^[23] and this might explain the leakage by ZnO without full

liposome disruption. Quite surprisingly, we cannot find any intact DOCP liposomes when it was mixed with ZnO (Figure 1J). At the same time, the ZnO surface had no lipid coating, while ZnO induced full DOCP leakage (Figure 2C). Taken together, we attribute this to the strong interaction between ZnO and the DOCP phosphate group, which fully disrupted the lipid membrane.

Based on the calcein leakage, cryo-TEM and ζ -potential data, we grouped these oxides into three types (Figure 1C–E). We also rationalize the grouping based on their surface properties. The seven type 1 oxides are all negatively charged, and this is also consistent with their point of zero charge (PZC) that has been reported (Supporting Information, Table S1).^[24] All these oxides are likely to interact with the liposomes through the lipid phosphate group.^[5,7,25] While both DOPC and DOCP have a phosphate, DOCP has a directly exposed phosphate that is not hindered by the choline group to allow full liposome wrapping.

The type 2 includes only SiO_2 , which leaked DOPC but not DOCP. While SiO_2 is also negatively charged, it has the lowest PZC value of less than 2, which makes phosphate binding very unfavorable at neutral pH. This might be a reason that silica uses mainly van der Waals force for lipid interactions.^[26] The special surface property of SiO_2 was noticed previously in the context of its strong surface acidity attributable to its bond strength to bond length ratio.^[27] The type 3 oxides include positively charged ZnO and NiO.^[28] They leaked both liposomes by membrane damage. Therefore, type 3 oxides might be more toxic to cells. Among these, the type 1 and 2 oxides are the most useful candidates for preparing supported lipid bilayers.

An inorganic core supporting a conformational bilayer membrane is a very useful construct.^[1] We next optimized the buffer conditions for the liposome wrapping reaction using Fe_3O_4 . Both Fe_3O_4 and DOCP liposomes are negatively charged at neutral pH, and we found that liposome wrapping was promoted at higher salt concentration, lower pH, while temperature has almost no effect from 25 to 45 °C (Supporting Information, Figure S9A–C). We proposed that the lipid phosphate is responsible for DOCP liposome wrapping, and this is supported by that free inorganic phosphate has an inhibition effect on calcein leakage (Supporting Information, Figure S9D). This is explained by the free phosphate capping the particle surface, thus competitively inhibiting DOCP liposome adsorption. Most previous work used hydrophobic ligands to cap magnetic NPs, and a phase transfer or ligand exchange reaction was required to bring the particles to the aqueous phase.^[11,18,29–32] Here, all the operations are carried out in an aqueous solution with a simple mixing step.

In the above work, we have profiled the oxides based on their lipid interactions, and established a general method to coat the type 1 oxides with a lipid bilayer. Furthermore, important insights regarding surface charge and chemical interactions were obtained. With a lipid envelope, many applications are possible.

In this initial study, we demonstrate bioconjugation on Fe_3O_4 and cellular uptake. We first tested cellular uptake using Fe_3O_4 NPs mixed with DOPC (Figure 3B) and DOCP (Figure 3C). Both liposomes contained 1% Rh label, and

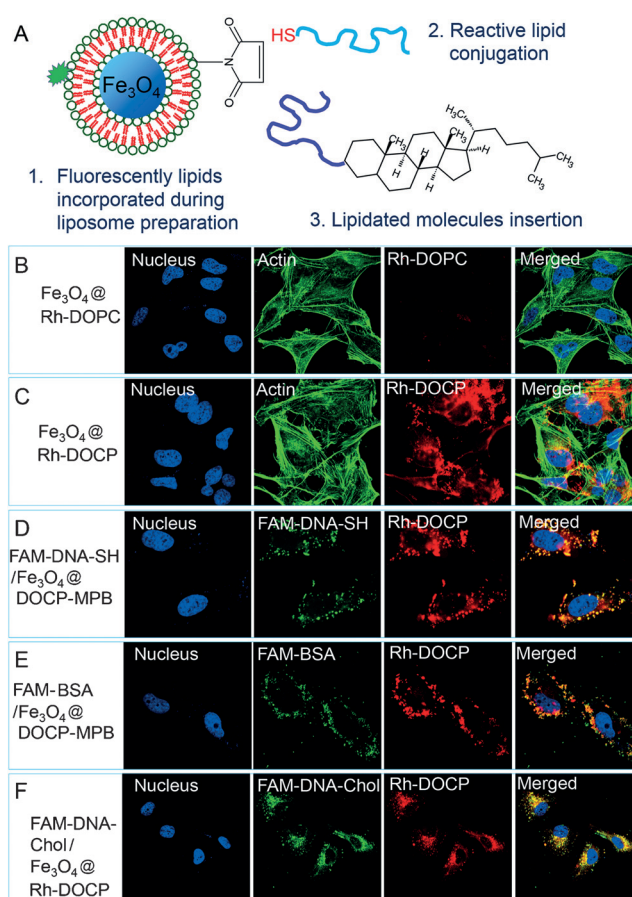


Figure 3. A) Three methods to conjugate ligands to Fe_3O_4 NP supported DOCP bilayer. Confocal fluorescence micrographs of B) Rh-DOCP/ Fe_3O_4 , and C) Rh-DOCP/ Fe_3O_4 internalized by HeLa cells. Internalization of D) FAM and thiol dual-labeled DNA, and E) FAM-labeled BSA conjugated to Fe_3O_4 supported DOCP containing 5% MPB-PE. F) Insertion of FAM and cholesterol dual labeled DNA into the Fe_3O_4 -supported DOCP membrane. Blue: cell nuclei; green: actin or FAM labels; red: Rh fluorescence indicating the lipids.

these labeled lipids can be directly incorporated during liposome preparation (Figure 3A, reaction 1). The DOCP conjugate showed much better cellular uptake. Compared to the normal PC lipid, the CP headgroup has a flipped dipole. It has been recently proposed that this flipped dipole might adhere strongly to the cell membrane,^[21] which might be a reason for its drastic uptake by cancer cells. Our quantitative ICP-MS measurement of the iron content confirmed that the DOCP coated Fe_3O_4 was internalized by about 60% more than the bare NP (Supporting Information, Figure S10). The biocompatibility of these materials were also measured. The DOPC and DOCP conjugates were not much different compared to the bare Fe_3O_4 in terms of toxicity (Supporting Information, Figure S11); all were highly biocompatible.

After studying cellular uptake, we next tested bioconjugation. Attaching ligands to iron oxide is not a simple task; it often involves organic solvents or coating another inorganic layer.^[10,11,16] With a lipid coating, we can readily achieve bioconjugation. For example, we incorporated a small fraction of the MPB-PE lipid (5%) into DOCP. Thus, molecules

with a free thiol can covalently attach to the maleimide group (Figure 3A, reaction 2). To demonstrate this, we employed a thiolated DNA and the bovine serum albumin (BSA) protein, both containing a carboxyfluorescein (FAM) label. When these conjugates were mixed with cells, strong green fluorescence from the DNA (Figure 3D) and BSA (Figure 3E) were observed, and they co-localized with the red lipid emission from the Rh label, suggesting these molecules were carried into the cells by the supported bilayers. The free DNA or BSA cannot be internalized by the cells (Supporting Information, Figure S12). This DNA construct is similar to the liposomal spherical nucleic acids by Mirkin and co-workers,^[33] but it contains a magnetic core that allows additional manipulation of the conjugate. Bioconjugation can also be readily achieved by direct insertion of lipid-modified molecules (Figure 3A, reaction 3). For example, we mixed the $\text{Fe}_3\text{O}_4/\text{DOCP}$ hybrid with a cholesterol and FAM dual labeled DNA, and efficient DNA uptake was also achieved (Figure 3F).

The above studies only showed the conjugation reactions without using the magnetic property of the core. Finally, magnetic separation was studied. We attached a cholesterol-TEG labeled A_{15} DNA to the conjugate. At saturation, about 600 DNAs were attached to each 30 nm Fe_3O_4 NP (Supporting Information, Figure S13). These particles were then added to a solution containing a mixture of two DNA:Alexa Fluoro 647 (AF)-labeled T_{15} (target DNA) and a FAM-labeled random DNA (rDNA). The initial fluorescence spectra showed strong emissions from both fluorophores (Figure 4B,

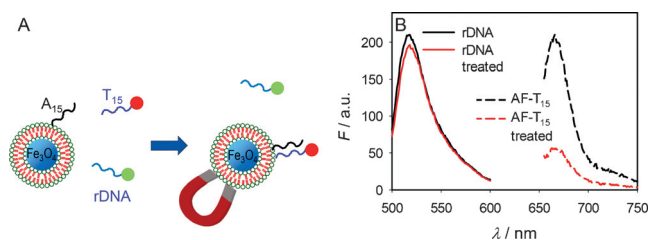


Figure 4. A) The magnetic separation of fluorescently labeled target DNA from a mixture. B) Fluorescence quantification of DNA separation based on (A).

black lines). After adding the NPs and magnetic separation, the AF emission was significantly reduced owing to its hybridization with the surface A_{15} , while the FAM emission was not affected (Figure 4B, red lines), suggesting successful DNA hybridization and magnetic separation. This experiment also indicates that DNA has maintained its molecular recognition function on the supported bilayer surface.

In summary, this work provides a general method for capping a number of important metal oxides with an engineered lipid bilayer. We obtained a comprehensive understanding on the interaction between various oxides and PC/CP liposomes, allowing us to classify the oxides into three types. Other than the cationic metal oxides, which damage lipid membranes, the rest can all form supported bilayers with either DOPC, or in most cases with DOCP liposomes. We further demonstrated a few applications of

magnetic iron oxide NPs enabled by the lipid envelope. Further work on improving NP colloidal stability and in vivo studies with targeting ligands will prove the full potential of this hybrid material. Compared to the previously reported methods for manipulating magnetic NPs, our method requires only a simple mixing step in an aqueous buffer. This simplified operation will likely enable more researchers to use this material for a diverse range of applications.

Acknowledgements

We thank R. Harris at the University of Guelph for assistance with cryo-TEM, and S.J. Hu at Waterloo for assistance with ICP-MS. Funding for this work is from the Natural Sciences and Engineering Research Council of Canada (NSERC), the National Natural Science Foundation of China (31571023, 81501587), and start-up funding from Hefei University of Technology.

Keywords: liposomes · magnetic nanoparticles · metal oxides · phosphocholine · supported bilayers

How to cite: *Angew. Chem. Int. Ed.* **2016**, *55*, 12063–12067
Angew. Chem. **2016**, *128*, 12242–12246

- [1] a) J. Liu, A. Stace-Naughton, X. Jiang, C. J. Brinker, *J. Am. Chem. Soc.* **2009**, *131*, 1354–1355; b) Y. S. Tu, M. Lv, P. Xiu, T. Huynh, M. Zhang, M. Castelli, Z. R. Liu, Q. Huang, C. H. Fan, H. P. Fang, R. H. Zhou, *Nat. Nanotechnol.* **2013**, *8*, 594–601; c) W. Gao, C.-M. J. Hu, R. H. Fang, L. Zhang, *J. Mater. Chem. B* **2013**, *1*, 6569–6585; d) S. Tan, X. Li, Y. Guo, Z. Zhang, *Nanoscale* **2012**, *5*, 860–872; e) J. Liu, *Langmuir* **2016**, *32*, 4393–4404.
- [2] C. E. Ashley, E. C. Carnes, G. K. Phillips, D. Padilla, P. N. Durfee, P. A. Brown, T. N. Hanna, J. Liu, B. Phillips, M. B. Carter, N. J. Carroll, X. Jiang, D. R. Dunphy, C. L. Willman, D. N. Petsev, D. G. Evans, A. N. Parikh, B. Chackerian, W. Wharton, D. S. Peabody, C. J. Brinker, *Nat. Mater.* **2011**, *10*, 389–397.
- [3] a) M. Mammen, S. K. Choi, G. M. Whitesides, *Angew. Chem. Int. Ed.* **1998**, *37*, 2754–2794; *Angew. Chem.* **1998**, *110*, 2908–2953; b) Y. Yang, J. Wang, H. Shigematsu, W. Xu, W. M. Shih, J. E. Rothman, C. Lin, *Nat. Chem.* **2016**, *8*, 476–483; c) T. D. MacDonald, T. W. Liu, G. Zheng, *Angew. Chem. Int. Ed.* **2014**, *53*, 6956–6959; *Angew. Chem.* **2014**, *126*, 7076–7079.
- [4] a) E. T. Castellana, P. S. Cremer, *Surf. Sci. Rep.* **2006**, *61*, 429–444; b) E. Sackmann, *Science* **1996**, *271*, 43–48; c) R. Michel, E. Kesselman, T. Plostica, D. Danino, M. Gradzielski, *Angew. Chem. Int. Ed.* **2014**, *53*, 12441–12445; *Angew. Chem.* **2014**, *126*, 12649–12653; d) A. N. Parikh, J. T. Groves, *MRS Bull.* **2006**, *31*, 507–512.
- [5] F. Wang, J. Liu, *Small* **2014**, *10*, 3927–3931.
- [6] E. Reimhult, F. Hook, B. Kasemo, *Langmuir* **2003**, *19*, 1681–1691.
- [7] F. Wang, J. Liu, *J. Am. Chem. Soc.* **2015**, *137*, 11736–11742.
- [8] A.-H. Lu, E. L. Salabas, F. Schueth, *Angew. Chem. Int. Ed.* **2007**, *46*, 1222–1244; *Angew. Chem.* **2007**, *119*, 1242–1266.
- [9] J. R. McCarthy, R. Weissleder, *Adv. Drug Delivery Rev.* **2008**, *60*, 1241–1251.
- [10] R. Hao, R. Xing, Z. Xu, Y. Hou, S. Gao, S. Sun, *Adv. Mater.* **2010**, *22*, 2729–2742.
- [11] W. J. M. Mulder, G. J. Strijkers, G. A. F. van Tilborg, A. W. Griffioen, K. Nicolay, *NMR Biomed.* **2006**, *19*, 142–164.

- [12] J. I. Cutler, D. Zheng, X. Xu, D. A. Giljohann, C. A. Mirkin, *Nano Lett.* **2010**, *10*, 1477–1480.
- [13] J. Li, C.-Y. Hong, S.-X. Wu, H. Liang, L.-P. Wang, G. Huang, X. Chen, H.-H. Yang, D. Shangguan, W. Tan, *J. Am. Chem. Soc.* **2015**, *137*, 11210–11213.
- [14] Z. Li, K. Dong, S. Huang, E. Ju, Z. Liu, M. Yin, J. Ren, X. Qu, *Adv. Funct. Mater.* **2014**, *24*, 3612–3620.
- [15] O. Sandre, C. Ménager, J. Prost, V. Cabuil, J. C. Bacri, A. Cebers, *Phys. Rev. E* **2000**, *62*, 3865–3870.
- [16] N. A. Frey, S. Peng, K. Cheng, S. Sun, *Chem. Soc. Rev.* **2009**, *38*, 2532–2542.
- [17] B. Dubertret, P. Skourides, D. J. Norris, V. Noireaux, A. H. Brivanlou, A. Libchaber, *Science* **2002**, *298*, 1759–1762.
- [18] M. De Cuyper, M. Joniau, *Eur. Biophys. J.* **1988**, *15*, 311–319.
- [19] M. D. Cuyper, P. Müller, H. Lueken, M. Hodenius, *J. Phys. Condens. Matter* **2003**, *15*, S1425.
- [20] E. K. Perttu, A. G. Kohli, F. C. Szoka, *J. Am. Chem. Soc.* **2012**, *134*, 4485–4488.
- [21] X. Yu, Z. Liu, J. Janzen, I. Chafeeva, S. Horte, W. Chen, R. K. Kainthan, J. N. Kizhakkedathu, D. E. Brooks, *Nat. Mater.* **2012**, *11*, 468–476.
- [22] S. Mornet, O. Lambert, E. Duguet, A. Brisson, *Nano Lett.* **2005**, *5*, 281–285.
- [23] P. R. Leroueil, S. A. Berry, K. Duthie, G. Han, V. M. Rotello, D. Q. McNerny, J. R. Baker, B. G. Orr, M. B. Banaszak Holl, *Nano Lett.* **2008**, *8*, 420–424.
- [24] M. Kosmulski, *J. Colloid Interface Sci.* **2002**, *253*, 77–87.
- [25] S. Wang, W. Morris, Y. Liu, C. M. McGuirk, Y. Zhou, J. T. Hupp, O. K. Farha, C. A. Mirkin, *Angew. Chem. Int. Ed.* **2015**, *54*, 14738–14742; *Angew. Chem.* **2015**, *127*, 14951–14955.
- [26] P. S. Cremer, S. G. Boxer, *J. Phys. Chem. B* **1999**, *103*, 2554–2559.
- [27] N. Sahai, *Environ. Sci. Technol.* **2002**, *36*, 445–452.
- [28] T. Mahmood, M. T. Saddique, A. Naeem, P. Westerhoff, S. Mustafa, A. Alum, *Ind. Eng. Chem. Res.* **2011**, *50*, 10017–10023.
- [29] M.-S. Martina, J.-P. Fortin, C. Ménager, O. Clément, G. Barratt, C. Grabielle-Madelmont, F. Gazeau, V. Cabuil, S. Lesieur, *J. Am. Chem. Soc.* **2005**, *127*, 10676–10685.
- [30] Y. Liu, T. Chen, C. Wu, L. Qiu, R. Hu, J. Li, S. Cansiz, L. Zhang, C. Cui, G. Zhu, M. You, T. Zhang, W. Tan, *J. Am. Chem. Soc.* **2014**, *136*, 12552–12555.
- [31] T. Chen, I. Öçsoy, Q. Yuan, R. Wang, M. You, Z. Zhao, E. Song, X. Zhang, W. Tan, *J. Am. Chem. Soc.* **2012**, *134*, 13164–13167.
- [32] S. Tong, S. Hou, B. Ren, Z. Zheng, G. Bao, *Nano Lett.* **2011**, *11*, 3720–3726.
- [33] R. J. Banga, N. Chernyak, S. P. Narayan, S. T. Nguyen, C. A. Mirkin, *J. Am. Chem. Soc.* **2014**, *136*, 9866–9869.

Received: July 7, 2016

Published online: August 19, 2016